Application of shock compression science to Earth and planetary physics

Thomas J. Ahrens

Citation: AIP Conference Proceedings **370**, 3 (1996); doi: 10.1063/1.50667
View online: http://dx.doi.org/10.1063/1.50667
View Table of Contents: http://scitation.aip.org/content/aip/proceeding/aipcp/370?ver=pdfcov
Published by the AIP Publishing

APPLICATION OF SHOCK COMPRESSION SCIENCE TO EARTH AND PLANETARY PHYSICS

Thomas J. Ahrens

Lindhurst Laboratory of Experimental Geophysics Seismological Laboratory, California Institute of Technology, Pasadena, CA 91125

After the development of shock compression methods for obtaining pressure-density Hugoniot curves, it became clear that these could be applied to both determining the equations-of-state and investigation of polymorphic phase changes in silicate minerals of planetary mantles and crusts, as well as, the iron alloys of the metallic cores of terrestrial planets. These data, when taken with seismological models of the Earth, yield constraints on the composition of the Earth's mantle and core. Shock data for molten silicates provide a basis for understanding the initial layering of a cooling terrestrial magma ocean. Application of shock-wave data is critical to delineating the energy partitioning upon hypervelocity impact on planetary surfaces, and permits calculation of the mass of melt and vapor produced by impactors as a function of impact velocity, as well as, providing a quantitative basis for determining the degree of erosion or accretion upon planetary impact as a function of impact and planetary escape velocity.

INTRODUCTION

Experimental and theoretical shock compression science has much to contribute to Earth and planetary science because of two fortunate coincidences:

(1) The range of impact velocities achievable with laboratory projectiles overlaps the escape velocity, V_e, and hence the infall velocity $V_e \leq 0.5$ km/sec for objects ranging in size ($<10^3$ km) for the asteroids and for the largest of the terrestrial planets (the Earth) $V_e = 11.2$ km/sec. Hence a wide range of problems dealing with the accretion of the planets via impact of asteroid-sized proto-planetesimals (Fig. 1) is possible within the framework of a now widely accepted Safronov-Kaula-Wetherill (SKW) accretion scenario.

These include the impact cratering process that represents the late stages of impact accretion. An extensive record of impact cratering is found on the Moon's surface. On the Earth, we now recognize ~120 impact craters, including the >200 km-diameter crater at Chicxulub, Mexico. The aftermath of the impact, which formed this crater, gave rise to the extinction preserved in the fossil record at the Cretaceous-Tertiary boundary, 65 million years ago. At this boundary, some 80% of the existing genera, became extinct. Recently, during the period of July 16 to 21, 1994 we observed, from ground and space-placed platforms, a similar energy event (10^{30} erg) upon impact (and accretion) of some 22 fragments of Comet Shoemaker-Levy 9 on Jupiter. This was an unusual event for the world's poplulation to witness, as its frequency is calculated to occur, only at intervals of, ~ 4,500 years [1].

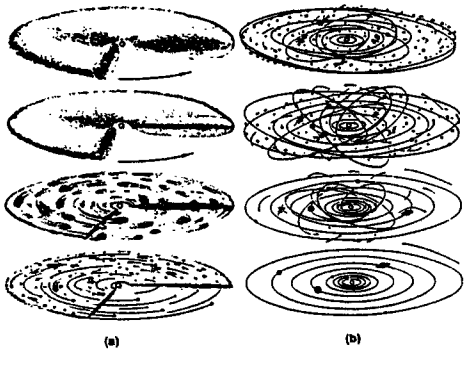

FIGURE 1 Solar system via Safronov-Wetherill-Kaula scenario. (a) Formation of asteroid-size intermediate bodies form dust component of solar nebula. (b) Runaway accretion to intermediate-sized bodies. Impact accretion of intermediate-sized bodies into planets. (After Levin, [17].)

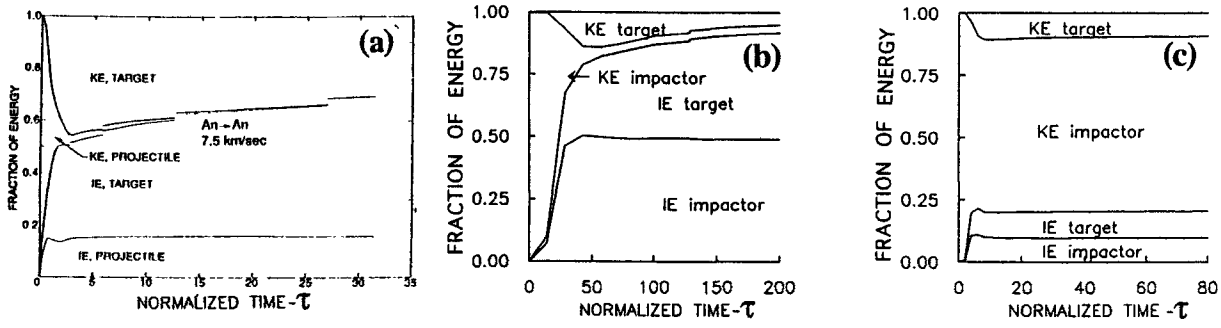

F IGURE 2. (a) Partitioning of energy versus τ for impact of 2.9 g/cm^3 anorthosite (An) projectile onto anorthosite planet. (b) for normal impact of 680 km radius projectile on 1700 km radius An object at 10 km/s. (c) for an oblique (50°) collision with a 1200 km (radius) impactor.

(2) The impact velocity of available explosive and gun-propelled impactors induces pressures and temperatures in Earth materials such that the whole range of pressures (364 GPa) and temperatures (6500 K) present in the Earth are achievable under dynamic compression conditions in the laboratory. All of the tools of shock-wave physics are available for determining the equations-of-state of Earth materials centered at normal, low-and high-temperatures. The resulting shock-wave data are applied with other mineral physics data to modeling of the Earth and planetary interiors.

Mineral physicists compare the properties of the Earth, as inferred from direct samples from depths of ~10^2 km, the present heat flow of the Earth and detailed elastic and density models of the Earth obtained with seismic waves to mineral properties as a function of temperature and pressure. Other properties of the Earth are obtained from the gravitational potential, monitoring current, and inferred past, variations in Earth rotation and variations in the magnetic field on time scales of ~10^2 to 10^{13} seconds. The latter provided information on the workings of the geodynamo, as-well-as, provide data on the variation of electrical conductivity within the Earth.

PLANETARY ACCRETION

Using a shock-wave equation-of-state derived from experiments conducted on a lunar sample, a gabbroic anorthosite [2] collected on the Apollo 16 Mission, we calculated the rather different energy budgets which result from normal and oblique impact of anorthosite projectiles onto a anorthosite planetary surface as shown in Fig. 2. In these plots we employ a normalized time, τ:

$$\tau = Ut/a \qquad (1)$$

where t is actual time, U is projectile velocity, and a is impactor radius.

An important feature of the SKW planetary accretion scenario is the simultaneous growth of planetesimals via impact accretion during the period (10^7 years) that the planets themselves accreted. Thus, the largest planetesimals accreted on the planets increased from ~1 km (diameter), (Fig. 1a), to ~10^3 km during the planetary formation period (Fig. 1b). During most of this time, the planets are covered with proto-atmospheres. For impact of a projectile onto such planets, once the projectile diameters exceed several atmospheric scale heights, the mass of ejecta is little affected by the presence of the atmosphere.

During accretion, planetesimals impact at velocities slightly in excess of the local escape velocity (Fig. 1). Impact of iron (Fe) and silicate (An) planetesimals (meteorites) on the planets demonstrate slightly varying accretion parity velocities. The accretion parity velocity, varies with planetary escape velocity (Fig. 3) along the line $M_e/M_m = 1.0$. Where M_e, which is a function of planetary escape velocity, is the cumulative mass of ejecta with velocities up to a given value of V_e, and, M_m is the projectile mass. For example, for impact on the Moon, which has escape velocity of 2.37 km/sec, impacts of either iron or anorthosite objects at speeds less than ~22 km/sec accrete material to the Moon whereas impacts at greater speeds, erode

more material than is accreted. At the planetary escape velocities for the Earth (11.2), Mars (5.03), and Mercury (4.17) impacts of An meteorites, at parity velocities occurs for impactor velocities of ~60, 45, and 37 km/sec. The accretion parity velocity is relatively insensitive to projectile type. We infer from Fig. 3 accretion parity occurs for Fe impactors on anorthosite at approximately 55, 42, 36, and 22 km/sec for large impactors on the Earth, Mars, Mercury, and the Moon, respectively.

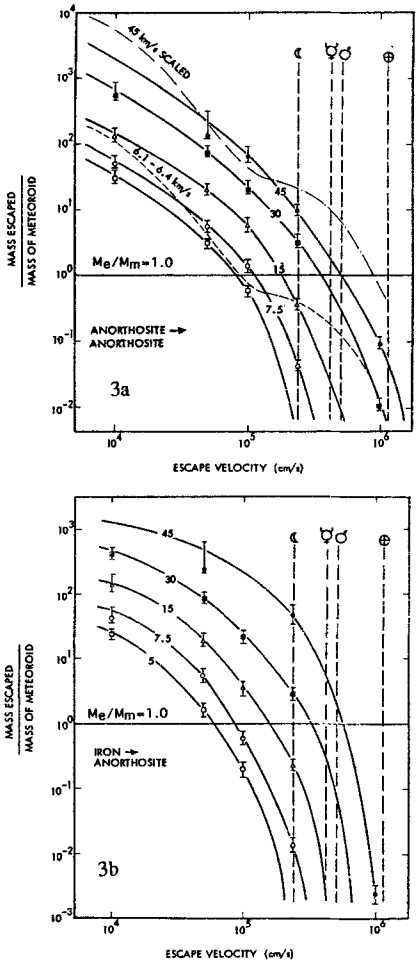

FIGURE 3. Cumulative (normalized) mass ejected at velocities, up to escape velocity (cm/sec) for impact of anorthosite (a) and iron (b) meteorites impacting onto anorthosite planets. Experimental data of Gault et al. [18] for 6.1-6.4 km/sec aluminum projectiles impacting basalt are extrapolated to 45 km/sec. Escape velocities for Moon, Mercury, Mars and Earth are indicated by vertical dashed lines (adapted from O'Keefe & Ahrens, [19]).

It is widely believed that the planetesimals which formed the terrestrial planets contained large inventories of the so-called atmophile (atmospheric) elements, that is, H, N, C plus the noble gases (He, Ne, Ar, Kr and Xe). The volatile-rich planetesimals are believed to have been similar to carbonaceous chondrite meteorites (e.g., Murchison meteorite)(Fig. 4a). Carbonaceous chondrites are believed to be samples of the C-class of asteroids. These objects contain typically several mm-diameter, spherical-shaped silicate "chondrules" and contain also, as a major component, carbon and hydrocarbons (including amino acids) up to 15%, by weight, H_2O mostly within a serpentine ($Mg_3Si_3O_7(OH)_4$)-like phase plus sulphates, nitrates, and iron-rich sulfide minerals. The results of shock recovery experiments on both the mineral, serpentine, and samples of carbonaceous chondrite meteorite (Murchison) indicate that impact velocities of ~2 km/sec and shock pressures of ~10 GPa are required to initiate devolatization of serpentine and serpentine-like phases in carbonaceous chondrites upon impact accretion. Impactors at velocities of 4 km/sec, induce shock pressures of 30 GPa, are required to complete devolatilized infalling planetesimals during impact accretion (Fig. 4a). For the case of the Earth, these impact velocities are achieved when it has grown to only 0.02 and 0.1 of its final mass (Fig. 4b), respectively.

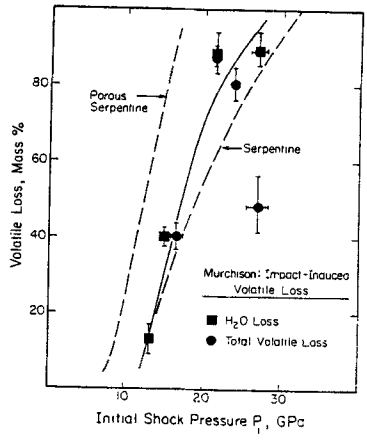

FIGURE 4 a. Shock-induced mass loss as a function of initial shock pressure for Murchison meteorite. Squares represent H_2O loss; circles total volatile loss. H_2O and total volatile loss are similar with the exception of one datum. Dashed lines are fits to data for impact-induced dehydration of 20% porous serpentine and crystal-density serpentine (from Tyburczy et al. [20]).

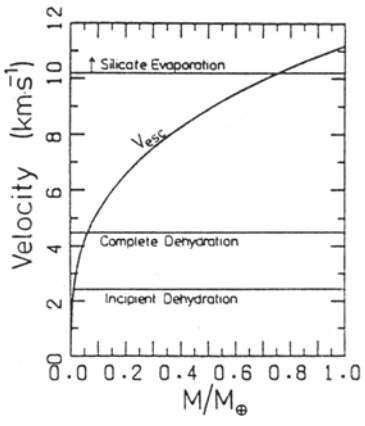

FIGURE 4b. Critical impact velocities for impact dehydration and vaporization, and excape velocities from proto-Earth are shown as a function of the mass of the proto-Earth, M, normalized by the present mass, $M_\oplus$. Impact velocities of planetesimals are approximated by escape velocity. Complete impact dehydration is expected at $M>0.1\ M_\oplus$ (from Abe, [21]).

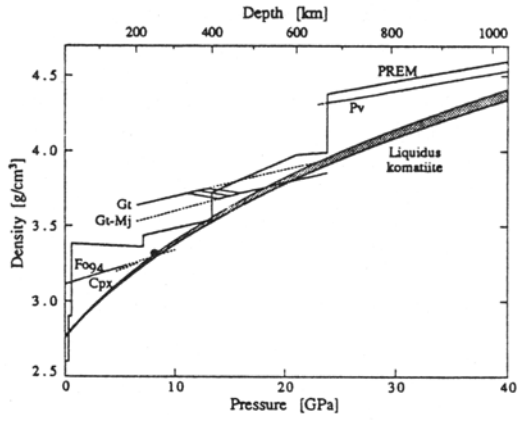

FIGURE 5 . Pressure-density relationships komatiite liquid and its liquidus phases along high-pressure liquidus. (Fo_{94}, olivine; Cpx, clinopyroxene; Gt, garnet; Gt-Mj, garnet-majorite; Pv, perovskite). Uncertainty in garnet to garnet-majorite transition is indicated by the hatched region. Dashed lines indicate solid phase densities at liquidus temperatures. Also shown, bulk mantle (PREM model [22]). Circle represents point of olivine neutral density calculated by Agee and Walker [7] at 8.1 GPa. Our data suggest that olivine would be neutrally buoyant near 8.2 GPa (252 km). (after Miller et al. [5]).

As the Earth continued to grow, the impact devolatized material from planetesimals, such as the carbonaceous chondrites, will have produced a massive, water-rich proto-atmosphere. Abe & Matsui [3] first pointed out that this will lead to a super-green house and a molten (magma) ocean covered Earth. In a green house, sunlight penetrates through the atmosphere (in the visible) but the thermal energy to be reradiated by the planetary surface is trapped because of the opacity in the infrared of the planetary atmosphere which contains CO_2 and H_2O. The super-green house is more severe. In this case projectiles, rather than sunlight, penetrate the atmosphere to deposit their energy on the planetary surface. The effect of the Sun only controls the temperature that the planet radiates to space (at the top of the atmosphere). Since for large impactors 60 to 90% of the energy of the impact is delivered as internal energy, to near-surface material, a molten (magma ocean) of silicate material forms. The major effect of the proto-atmosphere then is to provide an insulating blanket, capturing the heat flux, from impacted planetesimals. Late in the Earth's formation epic, impact of giant, lunar-sized planetesimals stripped-off the planet's proto-atmosphere [4].

We have conducted shock-wave experiments on a molten komatiite basalt composition - a molten silicate, rich in MgO, which approximates the liquid which would result from deep melting in the mantle [5]. The density of this liquid is such that in the upper mantle, crystals of olivine of composition, $(Mg_{0.94},Fe_{0.06})_2SiO_4$ will be neutrally buoyant in the molten magma ocean (Fig. 5). Neutral buoyancy of an olivine layer, at depths of 200 and 400 km, as demonstrated by this study, verifies theories proposed by Stolper et al. [6] and Agee and Walker [7] for the origin of the olivine-enriched upper mantle.

CORE COMPOSITION

Constraints on the composition of the outer liquid core are obtained by comparing shock-wave pressure-density and compressibility data at high pressure to Earth models. Birch [8] pointed out that the shock-wave data for Fe indicated that the outer, liquid, core of the Earth was less dense (by 10%) than iron in the 133 to 330 GPa pressure range. At pressures of 330-364 GPa, over the pressure range of the solid inner, core, a density close to that of pure iron matches models of the Earth. Several light elements, e.g. O, S, Si, and C, have been suggested as possible alloying elements, that upon dissolving in liquid iron in the outer core, can account for its lower density. In the case of oxygen, the shock-wave data for FeO (that has been demonstrated to undergo a transition to a metallic phase above 70 GPa [9] [10]) can be applied for this purpose. The

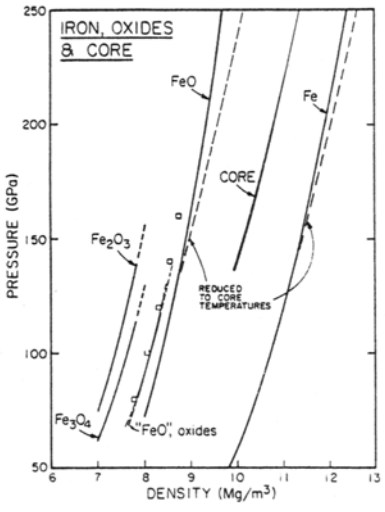

FIGURE 6. Shock-wave data for FeO , Fe , Fe_2O_3 and Fe_3O_4 (heavy curves) compared with seismologically determined compression curve of outer core. Fe and FeO data, corrected to core temperatures, are shown as thin dashed curves. Hugoniots of mixtures of oxides and Fe corresponding to FeO are given as thin curves: 1/3 (Fe + Fe_2O_3), 1/4(Fe + Fe_3O_4) and (Fe_3O_4 - Fe_2O_3), are plotted but overlap; open squares are from Al'tshuler & Sharipdzhanov [23]. Hugoniots for only high-pressure phase are shown. (after Jeanloz and Ahrens, [9]).

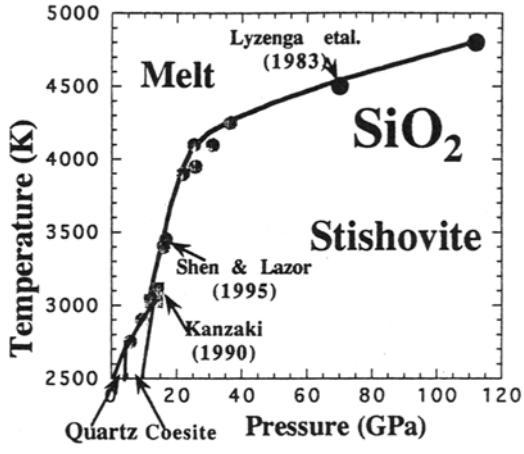

FIGURE 7. Phase diagram of SiO_2 from phase equilibrium studies and high-pressure, shock temperature study of Lyzenga et al. [13] that determined points on melting line of stishovite.

discovery of a transition in FeO to a metallic state allows more oxygen in models of the core than implied by previous data, and, both the density and bulk modulus versus pressure of the outer core is well represented by a mixture of 45 wt. % FeO (10 wt.% O) (Fig. 6).

SHOCK-WAVE TEMPERATURES

The very high-pressure phase of SiO_2, named stishovite, with a density of 4.35 g/cm^3 in which the Si^{+4} ion is in six-fold coordination with the O^{-2} ion , since discovery [11], is considered a prototype of the dense six-fold coordinated Si^{+4} structures in the Earth's lower mantle. The density of stishovite is high, relative to quartz (density, 2.65 g/cm^3), because of the increase in the Si-O coordination. Melting phenomena of mantle silicates, and the proto-type-stishovite, provide a firm upper-bound to the temperatures in the Earth, as well as, via the Weertman [12] relation between melting point and viscosity, provide a constraint to the quasi-static creep rheology of the mantle that controls convection.

Lyzenga et al. [13] reported the first-shock temperature measurements for SiO_2 (stishovite) and determined the melting behavior to 112 GPa and 4800K. Recently, static high-pressure, high-temperature, data for SiO_2 (stishovite) are reported to 36 GPa and 4300K (Fig. 7). These provide a growing and consistent data set for this key oxide.

CONCLUDING REMARKS

Shock wave research on Earth and planetary materials is an intellectually rich field, that also includes the equations-of-state and electrical properties of the constituents of the interiors of the major planets (e. g., Jupiter and Saturn) especially H_2, He, and H_2O [14]. Separate measurements of shock temperatures in metals and sound velocities in minerals and metals have also contributed to our understanding of planetary interiors. Another subject of interest is shock-induced tensile-and shear-damage in rock. This has an important bearing on the impact response of asteroids and planetary surfaces to impact cratering processes. Major impacts on terranes containing volatile-bearing minerals such as carbonates (Mg,Ca)CO_3 [15] and sulphates ($CaSO_4$) [16] release gases, such as CO_2 and SO_2 into the atmosphere. These strongly affect the Earth's climate. Giant impacts

appear to have played a major role in the evolution and extinction of species during the Earth's history.

ACKNOWLEDGMENTS

I am grateful to the collaboration of all of my students and colleagues and technical and administrative support personnel who I have worked with since 1962 in conducting my research, first, at Poulter Laboratory, Stanford Research Institute, and, later, the Seismological Laboratory's, Lindhurst Laboratory of Experimental Geophysics at at the California Institute of Technology. Supported by NSF, NASA and DOD. Contribution No. 5584.

REFERENCES

1. Takata, T., Ahrens, T. J., and Harris, A.W., *Geophys. Res. Lett.*, in press (1995).
2. Ahrens, T. J., O'Keefe, J. D., and Gibbbons, R. V., *Proc. IV Lunar Sci. Conf., Suppl. 4, Geochim. et Cosmochim. Acta*, **3**, 2575-2590 (1973).
3. Abe, y. and Matsui, T., *Proc. XVII Lunar and Planet. Sci. Conf., I, J. Geophys. Res.*, **91**, E291-E302 (1986).
4. Ahrens, T. J., *Physics Today*, **47**, 38-45 (1994).
5. Miller, G. H., Stolper, E. M., and Ahrens, T. J., *J. Geophys. Res.*, **96**, 11849-64 (1991).
6. Stolper, E. M., Walker, D., Hager, B. H., and Hays, J. F., *J. Geophys. Res.*, **86**, 6261-6271 (1981).
7. Agee, C. B., and Walker, D., *Earth Planet. Sci. Lett.*, **90**, 144-156 (1988).
8. Birch, F., *J. Geophys. Res.*, **69**, 4377-4388 (1964).
9. Jeanloz, R., and Ahrens, T. J., *Geophys. J. R. astr. Soc.*, **62**, 505-528 (1980).
10. Knittle, E., Jeanloz, R., Mitchell, A. C., and Nellis, W. J., *Sol. State Comm.*, **59**, 513-515 (1986).
11. Stishov, S. M., and Popova, S. V., *Geokhimiya*, **10**, 937-839 (1961).
12. Weertman, J., *Rev. Geoph. Space Phys.*, **8**, 145-168 (1970).
13. Lyzenga, G. A., Ahrens, T. J., and Mitchell, A. C., *J. Geophys. Res.*, **88**, 2431-2444 (1983).
14. Nellis, W. J., and Mitchell, A. C. in *Recent Trends in High Pressure Research- XIII AIRAPT Int. Conf. on High Pressure Sci. and Tech.*, New York, International Science Publisher, 1991, 487-491.
15. O'Keefe, J. D., and Ahrens, T. J., *Nature*, **338**, 247-249 (1989).
16. Chen, G., Tyburczy, J. A., and T.J. Ahrens, *Earth Planet. Sci. Lett.*, **128**, 615-628 (1994).
17. Levin, B. J., in *The Upper Mantle*, A. R. Ritsema (ed.), Elsevier, 1972, 7-30.
18. Gault, D. E., Shoemaker, E. M., and Moore, H. J., Spray ejected from the lunar surface by meteoroid impact, *NASA Tech. Note*, D-1767 (1963).
19. O'Keefe, J. D., and Ahrens, T. J., *Science*, **198**, 1249-1251 (1977).
20. Tyburczy, J. A., Frisch, B., and Ahrens, T. J., *Earth Planet. Sci. Lett.*, **80**, 201-207 (1986).
21. Abe, Y., *Lithos*, **30**, 223-235 (1993).
22. Dziewonski, A. M., and Anderson, D. L., *Phys. Earth Planet. Inter.*, **25**, 297-356 (1981).
23. Al'tshuler, L. V., and Sharipdzhanov, I. I., *Izv. Earth Phys., Engl. Transl.*, **3**, 167-177 (1971).